HHS Public Access

Author manuscript

Neuroimage. Author manuscript; available in PMC 2018 March 01.

Published in final edited form as:

Neuroimage. 2017 March 01; 148: 343–351. doi:10.1016/j.neuroimage.2017.01.045.

Regional and source-based patterns of [^{11}C]-(+)-PHNO binding potential reveal concurrent alterations in dopamine D_2 and D_3 receptor availability in cocaine-use disorder

Patrick D. Worhunsky, Ph.D.[a,b,*], **David Matuskey, M.D.**[a,b], **Jean-Dominique Gallezot, Ph.D.**[a], **Edward C. Gaiser, B.A.**[a,b], **Nabeel Nabulsi, Ph.D.**[a], **Gustavo A. Angarita, M.D.**[b], **Vince D. Calhoun, Ph.D.**[b,c,d], **Robert T. Malison, M.D.**[b], **Marc N. Potenza, M.D.**[b,e,f,g], and **Richard E. Carson, Ph.D.**[a]

[a]Department of Radiology & Biomedical Imaging, Yale School of Medicine, New Haven, CT, USA

[b]Department of Psychiatry, Yale School of Medicine, New Haven, CT, USA

[c]Department of Electrical & Computer Engineering, University of New Mexico, Albuquerque, NM, USA

[d]The Mind Research Network, Albuquerque, NM, USA

[e]Child Study Center, Yale School of Medicine, New Haven, CT, USA

[f]Department of Neuroscience, Yale School of Medicine, New Haven, CT, USA

[g]CASAColumbia, Yale School of Medicine, New Haven, CT, USA

Abstract

Dopamine type 2 and type 3 receptors (D_2R/D_3R) appear critical to addictive disorders. Cocaine-use disorder (CUD) is associated with lower D_2R availability and greater D_3R availability in regions primarily expressing D_2R or D_3R concentrations, respectively. However, these CUD-related alterations in D_2R and D_3R have not been concurrently detected using available dopaminergic radioligands. Furthermore, receptor availability in regions of mixed D_2R/D_3R concentration in CUD remains unclear. The current study aimed to extend investigations of CUD-related alterations in D_2R and D_3R availability using regional and source-based analyses of [^{11}C]-(+)-PHNO positron emission tomography (PET) of 26 individuals with CUD and 26 matched healthy comparison (HC) participants. Regional analysis detected greater binding potential (BP_{ND}) in CUD in the midbrain, consistent with prior [^{11}C]-(+)-PHNO research, and lower BP_{ND} in CUD in the dorsal striatum, consistent with research using non-selective D_2R/D_3R radiotracers. Exploratory independent component analysis (ICA) identified three sources of BP_{ND}

[*]*Corresponding author*: Patrick D. Worhunsky, Ph.D., Yale School of Medicine, 801 Howard Ave, New Haven, CT 06520; tel: 203-737-9738, fax: 203-785-3107, patrick.worhunsky@yale.edu.

Declaration of interest

The authors report that they have no financial conflicts of interest with respect to the content of this manuscript.

(striatopallidal, pallidonigral, and mesoaccumbens sources) that represent systems of brain regions displaying coherent variation in receptor availability. The striatopallidal source was associated with estimates of regional D_2R-related proportions of BP_{ND} (calculated using independent reports of [^{11}C]-(+)-PHNO receptor binding fractions), was lower in intensity in CUD and negatively associated with years of cocaine use. By comparison, the pallidonigral source was associated with estimates of regional D_3R distribution, was greater in intensity in CUD and positively associated with years of cocaine use. The current study extends previous D_2R/D_3R research in CUD, demonstrating both lower BP_{ND} in the D_2R-rich dorsal striatum and greater BP_{ND} in the D_3R-rich midbrain using a single radiotracer. In addition, exploratory ICA identified sources of [^{11}C]-(+)-PHNO BP_{ND} that were correlated with regional estimates of D_2R-related and D_3R-related proportions of BP_{ND}, were consistent with regional differences in CUD, and suggest receptor alterations in CUD may also be present in regions of mixed D_2R/D_3R concentration.

Keywords

cocaine use disorder; addiction; dopamine; striatum; independent component analysis; [^{11}C]-(+)-PHNO

1. Introduction

Individuals with cocaine-use disorder (CUD) exhibit alterations in subcortical dopamine including alterations in receptor availability, blunted dopamine release and reduced dopamine transport mechanisms (1–9). However, dopaminergic pharmacotherapies for stimulant-related addictions have displayed limited efficacy to date (see (10, 11)), thus a greater understanding of dopamine-related alterations in CUD may improve targeted interventions for addictions. Alterations in dopamine type-2 and type-3 receptors (D_2R/D_3R) are associated with CUD and other substance-use disorders (1–5, 12–17), suggesting related neurobiological mechanisms that may hold potential as targets in treating addictions. Specifically, D_2Rs and D_3Rs are implicated in the habitual and compulsive behaviors associated with the persistence of chronic drug use and relapse (18). Animal models demonstrate functional dissociation of D_2R and D_3R systems (19–21), suggesting these dopamine receptor subtypes may provide distinct contributions to addictive processes.

Research using dopamine-antagonist radioligands with equal affinities for D_2R and D_3Rs (e.g., [^{11}C]raclopride) indicate lower receptor availability in D_2R-rich striatal regions of individuals with CUD (1–5). By comparison, research using the D_3R-preferring dopamine-agonist radioligand [^{11}C]-(+)-PHNO in CUD and stimulant addiction indicate increased receptor availability in the D_3R-rich midbrain (8, 9, 22). These concurrently upregulated and downregulated dopamine systems in CUD may undermine dopaminergic therapies for cocaine addiction. Adding to this complexity, D_2R and D_3R are both expressed in structures central to addiction (e.g., midbrain, ventral striatum, pallidum) (23), and assessing potential alterations of specific receptor subtypes in these regions is challenging.

Regional binding of [^{11}C]-(+)-PHNO reflects local concentrations of both D_2Rs and D_3Rs (24, 25), allowing for simultaneous imaging of D_2R/D_3R not possible using other D_2-like receptor radioligands. To date however, [^{11}C]-(+)-PHNO research of CUD has not replicated

findings of lower receptor availability in the D_2R-rich dorsal striatum, or detected alterations in mixed-D_2R/D_3R regions (8, 9). However, these results of non-altered D_2R-like availability in the striatum in CUD are consistent with research using alternative dopamine-agonist radioligands with equal affinities for D_2R/D_3R (e.g., [^{11}C]NPA)(26). The current study aimed to further examine D_2R and D_3R alterations in the midbrain, striatum and other subcortical structures (e.g., globus pallidus, ventral pallidum and hypothalamus) in CUD using [^{11}C]-(+)-PHNO positron emission tomography (PET) imaging. Investigation of regional [^{11}C]-(+)-PHNO BP_{ND} was conducted on individuals with CUD and matched healthy comparison (HC) participants.

In addition, exploratory spatial independent component analysis (ICA) was performed on [^{11}C]-(+)-PHNO BP_{ND} data to examine D_2R and D_3R using a source-based approach. ICA is a data-driven computational procedure that decomposes or 'un-mixes' a measured signal into its maximal spatially independent 'sources'. While [^{11}C]-(+)-PHNO exhibits an estimated 20- to 50-fold selectivity *in vivo* for D_3Rs relative to D_2Rs (27–29), local BP_{ND} reflects a weighted sum of D_2R/D_3R concentrations. That is, [^{11}C]-(+)-PHNO BP_{ND} primarily reflects D_3R availability in D_3-rich regions (e.g., substantia nigra), D_2R availability in D_2-rich regions (e.g., dorsal striatum), and an aggregate of D_2R and D_3R availability in mixed D_2R/D_3R regions (e.g. ventral striatum) (24, 25, 30, 31). This unique mixed-signal nature of [^{11}C]-(+)-PHNO strongly motivates the utility of source-based analyses like ICA to un-mix the D_2R and D_3R components of BP_{ND} and examine distinct sources of receptor availability.

We hypothesized that CUD-related reductions in D_2R availability in the dorsal striatum would be detectable using [^{11}C]-(+)-PHNO in a large sample, and that CUD-related increases in D_3R availability in the midbrain would be confirmed. We also hypothesized that the exploratory ICA would identify sources of [^{11}C]-(+)-PHNO BP_{ND} consistent with estimates of regional proportions of D_2R-related and D_3R-related BP_{ND}, with mixed-D_2R/D_3R regions incorporated into multiple sources. Consistent with research demonstrating regional differences in D_2R and D_3R in CUD, we hypothesized that individuals with CUD would exhibit increased intensity of sources that include D_3-rich regions and reduced intensity of sources that include D_2-rich regions. Finally, we examined relationships between regional BP_{ND} and source intensities with duration of cocaine use.

2. Methods and Materials

2.1. Participants

Participants were 26 non-treatment seeking individuals with CUD and 26 age- and gender-matched HC participants, most of whom (22 CUD and 21 HC) were included in previous reports (8, 32) (Table 1). Physical exams with medical history, routine laboratory studies, pregnancy tests and electrocardiograms (ECGs) were performed to assess medical health eligibility criteria. Urine toxicology screening for a range of drugs (including cocaine, amphetamines, marijuana, opiates, benzodiazepines, barbiturates) were performed to confirm cocaine-use status in CUD participants and the absence of other recent drug use in both CUD and HC participants. Participants were assessed for DSM-IV diagnoses using clinical interviews (SCID (33); MINI (34)). Participants meeting criteria for cocaine

dependence (i.e., presenting with 3 or more criteria) were included in the CUD sample. Exclusion criteria included the presence or history of a general medical illness or psychotic disorder, pregnancy or breast feeding, or any condition that would interfere with the ability to participate in PET or MRI protocols (e.g., claustrophobia, metallic implants). All study procedures were approved by the Yale Human Investigation, Yale University Radiation Safety, Yale-New Haven Hospital Radioactive Drug Research, and Yale MRI Safety Committees, and participants provided written informed consent.

2.2. Radiochemistry and image acquisition

[^{11}C]-(+)-PHNO was prepared as previously described (35, 36). Radioactive dose, specific activity and injected mass for CUD and HC groups are listed in Table 1. PET imaging was performed on a Siemens high-resolution research tomograph (HRRT; Siemens/CTI, Knoxville, TN, USA). A transmission scan was obtained before the emission scan. PET scans (slices=207, slice separation=1.2mm, reconstructed image resolution ~3 mm) were acquired for 120 min at rest. Head motion was measured using an optical detector (Vicra, NDI Systems, Waterloo, Ontario, Canada). MR images were collected on a Siemens 3T Trio system (Siemens Medical Solutions, Malvern, PA) using a magnetization prepared rapid acquisition gradient echo (MPRAGE) sequence (repeat time (TR)/echo time (TE)=2530/3.34, flip angle=7°, in-plane resolution=0.98×0.98 mm, matrix=256×256, slice thickness=1mm, slices=176).

2.3. Image processing

Dynamic PET data (frame timing: 6×30s; 3×60s; 2×120s; 22×300s) were reconstructed with corrections (attenuation, normalization, scatter, randoms, deadtime and motion) using the MOLAR algorithm (37). Parametric images of [^{11}C]-(+)-PHNO BP_{ND} were computed using a simplified reference tissue model (SRTM2 (38)) with the cerebellum as reference (39). Registration of individual images into MNI152 space (40) was performed using SPM12 (Wellcome Trust Centre for Neuroimaging, London, UK). A summed [^{11}C]-(+)-PHNO uptake (0–10 min post-injection) image was created from the motion-corrected PET data and rigid-body registered to the subject's MR image. Nonlinear registration of the MR image to MNI152 space was determined using optimized unified segmentation (41). The combined rigid-body and nonlinear registrations were applied to the parametric BP_{ND}, and smoothed with a 4mm FWHM Gaussian kernel.

2.4. Analyses of regional [^{11}C]-(+)-PHNO BP_{ND}

Seven regions of interest (ROIs) were examined: dorsal caudate (DCA), dorsal putamen (DPU), globus pallidus (GP), hypothalamus (HY), substantia nigra (SN), ventral pallidum (VP), and ventral striatum (VS). ROIs were defined using previously described guidelines (24, 42). DCA, DPU and VS ROIs were obtained from FSL (Oxford Centre for Functional MRI of the Brain, Oxford, UK (24)). GP, HY, and VP ROIs were manually drawn on the ICBM-MNI52 template (Montreal Neurological Institute, Montreal, Canada). The SN ROI was manually defined on a group-average parametric [^{11}C]-(+)-PHNO BP_{ND} image from an independent sample (35). Regional [^{11}C]-(+)-PHNO BP_{ND} was determined from the individual smoothed parametric BP_{ND} images in standard space. ROI volumes were calculated by inverse transformation of template regions into individual native space. A

confirmatory whole-brain, between-group analysis was performed on BP_{ND} images using a two-sample t-test in SPM12 with a relative threshold mask (0.8; displayed in Figure 1). Due to the relatively low BP_{ND} signal (less than 0.5) in the thalamic and amygdala regions included in previous reports, substantial portions of these structures did not survive threshold masking and thus were excluded from ROI analyses. Group differences were explored at an uncorrected significance level of $p<0.005$, and cluster extent (k) >20 contiguous voxels.

2.5. Independent component analysis (ICA)

Exploratory ICA was performed on parametric images of [^{11}C]-(+)-PHNO BP_{ND} using the source-based morphometry (SBM (43)) module of the Group ICA of fMRI Toolbox (GIFT v2.0e; http://mialab.mrn.org/software/gift). Using higher order statistics, ICA identifies maximally independent vectors that comprise an unknown linear mixture (A) of mostly non-Gaussian sources (s) that generate a random variable (x). Given $x = As$, ICA solves for $y = Wx$, or the estimated un-mixing matrix (W) of approximated source maps (y). Parametric images of all 52 participants were entered into the ICA to allow direct comparison of source loadings. The analysis was constrained to data within the relative threshold mask determined in the GLM analysis (described above), and with no prior information as to group membership. A modified minimum-description-length (MDL) criterion (44) estimated the dimensionality of the dataset to consist of three sources which were extracted from the aggregate dataset using a neural-network algorithm designed to minimize mutual information of source outputs (InfoMax (45)).

Output from the ICA included the spatial source maps (y_M; M =1,2,3) and subject ICA-loading values ($\tilde{A}$; $1_{M,i}$; i = 1, …, 52), where $\tilde{A}$ denotes the estimate of the unknown mixing matrix A (i.e. the inverse of ICA-derived un-mixing matrix W). Note that applications of ICA to biomedical images typically employ principal component analysis (PCA) for data reduction prior to ICA; thus, subject ICA-loadings also incorporate the PCA-reduction factor (R) and are more accurately characterized as ($R \times \tilde{A}$), but for convenience, we use $\tilde{A}$ to represent the final subject ICA-loading parameters. The subject ICA-loading values represent the source 'intensity' or relative strength to which each subject's BP_{ND} data contained a given source. The spatial source maps were 'intensity-scaled' such that ($y_M \times \tilde{A}$) reflects the relative contribution of each source to the aggregate BP_{ND} signal, where $\tilde{A}_{M,i}$ is the average subject intensity for source M, and:

$$\tilde{x} = (y_1 \times \tilde{A}_{1,i}) + (y_2 \times \tilde{A}_{2,i}) + (y_3 \times \tilde{A}_{3,i}) + \overline{x}$$

where $\tilde{x}$ is the approximate reconstruction of the original data x, and $\overline{x}$ is the global mean BP_{ND} value (1.56) removed prior to ICA extraction. For analysis purposes, the source maps were scaled to ICA-estimated BP_{ND} ($\tilde{BP}_M$) through the product of ($y_M \times \tilde{A}_{M,i}$). For display and anatomical assignment purposes, the scaled source maps were thresholded at $\tilde{BP}_M \geq 0.5$ (with no cluster-extent threshold) based on the relevant range of [^{11}C]-(+)-PHNO BP_{ND} of 1.5–4.

To examine source compositions relative to regional estimates of D_2R/D_3R availability, intensity-scaled source maps were generated for all subjects, and regional $\tilde{BP}_M$ values were

extracted from the seven ROIs and compared the D_2R-related and D_3R-related proportions of BP_{ND} calculated using reported regional fractions of [^{11}C]-(+)-PHNO BP_{ND} (24, 25). That is, regional BP_{ND} values obtained in the ROI-based analysis (see Section 2.4. and Figure 1) were multiplied by average D_2R-and D_3R-related fractions reported in (23, 24) (Supplementary Table 1) to obtain regional estimates of local D_2R/D_3R BP_{ND} (i.e., $BP_{ND}^{D2}=BP_{ND} \times f_{D2}; BP_{ND}^{D3}=BP_{ND} \times f_{D3}$). Average regional $\tilde{B}P_M$ for each source were then examined in relation to the calculated estimates of BP_{ND}^{D2} and BP_{ND}^{D3} using Pearson correlations to assess potential association with D_2R-related and D_3R-related BP_{ND} proportions.

2.6. Statistical procedures

Group differences in ROI BP_{ND} values and ICA source intensities were assessed with two separate multivariate analyses of variance (i.e., group × ROI and group × source) and post-hoc univariate analyses. Due to non-tracer conditions of [^{11}C]-(+)-PHNO for D_3Rs at the administered dose (25), multivariate analyses including the estimated free concentration of [^{11}C]-(+)-PHNO (based on the average mass concentration in the cerebellum from 90–120 mins, multiplied by the specific activity) as a covariate were performed and revealed no significant mass dose effect on results (p's>0.4). Given reported associations between [^{11}C]-(+)-PHNO BP_{ND} and age and body-mass (46–48), all between-group multivariate and univariate analyses were repeated adjusting for age and body-mass. Additional analyses were performed to examine potential influences of alcohol use across all participants (12, 13) and cigarette smoking (14) within CUD participants. Exploratory correlational analyses were performed to examine relationships between regional and source-based binding measures with years of cocaine use.

3. Results

Participant characteristics and radioactivity information are provided in Table 1. There were no group differences in body-mass or radiotracer injection parameters. CUD participants were more likely to be daily tobacco smokers (χ^2=32.4, p<0.001) and did not differ from HCs in weekly alcohol consumption. ROI volumes (in subject/native space) did not differ between groups (p's>0.1).

3.1. Regional analyses of [^{11}C]-(+)-PHNO BP_{ND}

Results of ROI and whole-brain analyses are displayed in Figure 1. There was a main effect of group across ROIs ($F_{7,44}$=3.87, p=0.002), with CUD relative to HC displaying greater BP_{ND} in the SN (t_{50}=2.91, p=0.005) and lower BP_{ND} in the DPU (t_{50}=2.14, p=0.037), while a group difference in the DCA did not reach significance (t_{50}=1.79, p=0.080) (Figure 1a). Whole-brain analysis confirmed CUD relative to HC participants exhibited greater BP_{ND} in the midbrain and lower BP_{ND} in the dorsal striatum (Figure 1b). Consistent with previous reports (46, 48, 49), there was a significant association between age and BP_{ND} ($F_{7,42}$=3.25, p=0.008), and a marginal association between body-mass and BP_{ND} ($F_{7,42}$=2.23, p=0.051). Adjusting for influences of age and body-mass, group differences in the SN remained significant ($F_{1,48}$=11.29, p=0.002) while differences in the DPU did not reach significance

($F_{1,48}$=3.72, p=0.060). There was no main effect of alcohol use on BP_{ND} ($F_{7,44}$=0.87, p=0.54), and group differences survived adjusting for the number of cigarettes smoked daily ($F_{7,43}$=3.89, p=0.002). Within CUD participants, there was no association between BP_{ND} and daily cigarettes smoked ($F_{7,18}$=0.55, p=0.79) or years of cocaine use ($F_{7,18}$=1.07, p=0.42).

3.2. ICA of [^{11}C]-(+)-PHNO BP_{ND}

The exploratory ICA identified three sources of [^{11}C]-(+)-PHNO binding that represent systems of brain regions displaying coherent variation in BP_{ND} through the sample (Figure 2; Table 2). Source 1 represented a 'striatopallidal source', with largest contributions in the DPU, DCA, GP, VP and VS. Source 2 represented a 'pallidonigral source' comprised of the SN, GP, VP and HY. Source 3 represented a ventral 'mesoaccumbens source' encompassing HY, VP, VS and anterior regions of the midbrain extending into the SN. Although extracted solely from the data, the identified sources were spatially consistent with the distribution of D_2R-related and D_3R-related availability across regions of interest (Figure 3). Specifically, regional $\tilde{B}P_M$ values of the striatopallidal source were associated with estimated D_2R-related BP_{ND} proportions (r=0.89, p=0.008), and regional $\tilde{B}P_M$ of the pallidonigral source were associated with estimated D_3R-related BP_{ND} proportions (r=0.89, p=0.007). The mesoaccumbens source was not associated with either D_2R-related or D_3R-related binding proportions (p's>0.1).

ICA subject intensities for the three sources did not correlate with each other (p's>0.2). There were no associations between source intensities and age ($F_{3,46}$=1.53, p=0.22) or body-mass $F_{3,46}$=1.80, p=0.16). There was no main effect of alcohol use on source intensities ($F_{3,46}$=1.48, p=0.23).

3.3. [^{11}C]-(+)-PHNO BP_{ND} sources and CUD

There was a main effect of group on ICA-intensity across the three identified sources ($F_{3,48}$=4.28, p=0.009). CUD relative to HC participants displayed lower intensities of the striatopallidal source (t_{50}=2.58, p=0.013; Figure 3a) and greater intensity of the pallidonigral source (t_{50}=2.03, p=0.047; Figure 3b). Group differences in the mesoaccumbens source did not reach significance (t_{50}=1.63, p=0.109). Different from the regional analysis above, the intensity of the striatopallidal source was negatively associated with years of cocaine use (r=0.39, p=0.048; Figure 3a) and pallidonigral source intensity was positively correlated with years of cocaine use (r=0.40, p=0.042; Figure 3b). Group differences survived adjusting for the number of cigarettes smoked daily ($F_{3,47}$=4.28, p=0.009), and within CUD participants there was no association between source intensities and the number of cigarettes smoked daily ($F_{3,22}$=0.75, p=0.53).

4. Discussion

The current study extends prior research of D_2R/D_3R availability in CUD using [^{11}C]-(+)-PHNO. Regional analyses revealed CUD-related dorsal striatal reductions in D_2R-related BP_{ND}, consistent with D_2R/D_3Rantagonist radioligand research (1–5) but not previously detected with the D_3R-preferring [^{11}C]-(+)-PHNO, and confirmed greater availability in the

SN in CUD (8, 9). Exploratory ICA identified three sources of [^{11}C]-(+)-PHNO BP_{ND} that were correlated with regional proportions of D_2R-related and D_3R-related BP_{ND} and spatially consistent with known subcortical dopamine circuitry. Individuals with CUD relative to HC exhibited reduced intensity of a D_2R-related striatopallidal source and greater intensity of a D_3R-related pallidonigral source that were both associated with years of cocaine use, an association not found when analyzing regions individually. Notably, the ICA-identified sources suggest CUD-related alterations may be present in regions of mixed D_2R/D_3R concentration (e.g., ventral striatum, globus pallidus) not previously observed using traditional analyses of D_2R/D_3R radioligands. The current findings underscore the advantage of [^{11}C]-(+)-PHNO in simultaneous investigation of both D_2R and D_3R alterations in addictions, especially when combined with ICA in exploring sources of dopamine receptor availability. The patterns of concurrently increased and decreased receptor availability, particularly within structures (e.g., the ventral striatum), lend insight into the clinical challenges of dopaminergic pharmacotherapy for CUD.

4.1. Regional [^{11}C]-(+)-PHNO BP_{ND} in CUD

Alterations in D_2-like receptor systems in CUD have been reported using multiple radioligands, and the current ROI and whole-brain observations of greater midbrain and reduced dorsal striatal BP_{ND} are consistent with previous research (1–5, 8, 9). Reduced D_2R-related BP_{ND} in the striatum and greater D_3R-related BP_{ND} in the SN and have been linked to increased impulsivity in cocaine/stimulant addictions (9, 50). Lower striatal D_2R BP_{ND} has been associated with poor behavioral therapy outcomes in CUD (51). The relationship between reduced striatal BP_{ND} and years of cocaine use in the current study is consistent with preclinical evidence of the effects of cocaine exposure on D_2R availability (52). Similarly, increases in D_3R systems follow cocaine exposure in animal models (53, 54), though the previous finding of a relationship between D_3R-related SN BP_{ND} and years of cocaine use (8) was not replicated in the current regional analysis. Dissociating potential dopaminergic vulnerabilities to addictive disorders and dopaminergic consequences of substance use remains an important area of addictions research (55).

4.2. Sources of [^{11}C]-(+)-PHNO BP_{ND}

ICA identified three sources of [^{11}C]-(+)-PHNO BP_{ND} that were correlated with estimated regional proportions of D_2R-related and D_3R-related BP_{ND} and spatially consistent with dopamine circuitry. The striatopallidal source was identified in nodes of the ‘indirect’ dopamine pathway linking the striatum (DPU, DCA and VS) to the SN through connections with the pallidum (GP and VP). The indirect pathway is comprised of D_2R-expressing GABAergic medium spiny neurons interconnecting the striatum and pallidum. Consistent with this indirect pathway anatomy, the intensity of the identified striatopallidal source was strongly associated with estimated regional D_2R components of [^{11}C]-(+)-PHNO BP_{ND} (24, 25). Preclinical models indicate striatopallidal D_2R mechanisms may counterbalance reward-related responsivity, with impaired functioning associated with a greater sensitivity to drug-related rewards (56). Evidence also suggests a role of indirect-pathway striatal D_2R with behavioral inflexibility relative to aversive conditions (57, 58) and compulsive cocaine-seeking (59).

The pallidonigral source identified by ICA was composed of regions highly correlated with estimates of regional proportions of D_3R [^{11}C]-(+)-PHNO BP_{ND} (24, 25). The pallidonigral source is spatially consistent with dopamine circuitry between the pallidal structures and the midbrain. While less is understood regarding specific functionality of D_3R systems, integration of GP, VP and SN regions suggest a role of this system in drug-related reinforcement processing and motivational/appetitive states (60). Incentive salience models of addiction identify 'wanting' as a motivation state, dissociable from the hedonic state of 'liking', as a process that becomes sensitized over the course of an addiction (61), and is associated with greater D_3R availability in the SN in polysubstance and methamphetamine users (17, 22).

The mesoaccumbens source was identified in SN, VS and VP regions. While the SN and VP are D_3R-rich regions, there was no relationship between regional source intensities and estimated D_3R-related (or D3R-related) proportions of [^{11}C]-(+)-PHNO BP_{ND} across ROIs. Decreased D_2R/D_3R availability in the SN and VS is associated with increased sensitivity to reinforcing effects of stimulants mediated through increased striatal dopamine release (62). Neuroadaptive increases in SN and VS D_3R associated with cocaine exposure (54, 63) may act to downregulate the stimulant-induced release of dopamine in the striatum in individuals with CUD (4, 5). While a functional role of D_2R/D_3R in VS and midbrain circuitry appears critical in balancing dopamine transmission in CUD, mesoaccumbens source intensities were not altered in CUD (or associated with years of cocaine use), and additional research and/or validation of the reliability of this source is warranted.

4.3. Clinical implications of D_2-like receptor sources in addictive disorders

CUD-related differences in source intensities were consistent with regional analyses, broadly identifying lower D_2R-related and greater D_3R-related source intensities. ICA-identified sources extend individual regional observations, detecting CUD-related differences in regions characterized by mixed-D_2R/D_3R concentrations. Patterns of source-intensity difference suggest concurrent upregulation and downregulation of receptor availability in the VS and pallidal regions. In the current study, alterations in striatopallidal and pallidonigral sources, proposed to reflect complementary mechanisms of the indirect dopamine pathway, were associated with years of cocaine use. The intensities of these two sources were significantly related to CUD chronicity, suggesting receptor alterations may represent reciprocal compensatory adaptations through the course of addiction.

Despite extensive efforts to identify effective pharmacotherapies for CUD, there is currently no FDA-approved medication with an indication for CUD. Although it has been proposed that dopamine-agonist therapies may aid in the maintenance of cocaine abstinence (64), preclinical evidence of the influences of D_2R and D_3R agonists and antagonists on cocaine-related behaviors is mixed (65–68). The current findings illustrate the underlying complexity of targeting receptor subtypes that may integrate into multiple functional systems and influence drug-related behavior differently depending on the region of action (69). Adding to the challenge of dopaminergic pharmacotherapies are the neuroplastic adaptations associated with cocaine exposure and chronic use, suggesting dopaminergic interventions may be

aimed at ‘moving targets’, resulting in heterogeneous response profiles across individuals at different stages of addiction.

4.4. Strengths and limitations

The current study investigated the largest sample of CUD participants completing [^{11}C]-(+)-PHNO PET to date (N=26 relative to previous samples that included 10 to 16 individuals (8, 9, 32)), and demonstrates [^{11}C]-(+)-PHNO sensitivity to reductions in dorsal striatal D_2R availability frequently reported in CUD using equal-affinity D_2R/D_3R antagonist radioligands. The current sample was largely comprised of previously reported subjects. ROI results of CUD-related BP_{ND} alterations in the DPU survived post-hoc analysis co-varying for cohort (p=0.03), suggesting greater statistical power (rather than potential differences in individual variability across independent cohorts) contributed to the significant detection of D_2R-related differences in individuals with CUD. This study also represents the first application of ICA to explore sources of covarying D_2R/D_3R availability and examine alterations associated with CUD.

The data-driven ICA extraction was blind to the spatial distributions of D_2R/D_3R concentrations and blind to subject group assignments. The current mixed-sample design, while allowing direct comparison of source intensities in CUD relative to HC, identified three sources of [^{11}C]-(+)-PHNO BP_{ND} and alternative strategies of component extraction (e.g., higher-dimension ICA) may identify alternative sources (70). Alternative computational strategies (e.g., principal component analysis; PCA) have also been used to investigate PET data using ROI-based and voxel-wise approaches (71, 72), and may identify different factor structures in [^{11}C]-(+)-PHNO data.

Proposed associations with D_2R-related and D_3R-related availability in identified sources were based on calculated estimates using fractions of D_3R-related [^{11}C]-(+)-PHNO BP_{ND} derived in healthy controls using antagonists that are not 100% selective for D_3R receptors (24, 25). Thus, imprecise estimates, and potentially altered regional D_2R/D_3R-related fractions in individuals with CUD, limit conclusive determination of source signals relative to receptor subtypes. Research using ICA in conjunction with specific D_2R and D_3R blocking agents would be needed to validate these exploratory source compositions. Similarly, interpretations of potential functional involvement of identified sources was based on spatial patterns of regional integration relative to the extant and evolving literature, and direct examination of source relationships with measures of impulsivity, compulsivity, and substance use-related domains (e.g., self-administration, craving and cue-reactivity) may reveal alternative associations. Potential influences of co-occurring nicotine dependence in CUD participants on D_2R/D_3R availability warrants consideration given group differences in regular tobacco smoking (14). Though daily smoking amounts were not associated with PET results within CUD participants, future studies including a nicotine-dependent comparison sample would allow examination of cocaine-specific alterations in D_2R/D_3R receptor systems. Additional research is needed to replicate current observations and explore these dopamine systems in other addictive disorders.

4.5. Conclusions

The current study extends previous research of regional D_2R/D_3R availability in CUD measured with [^{11}C]-(+)-PHNO, detecting lower BP_{ND} the dorsal striatum and replicating greater BP_{ND} in the midbrain. Source-based analysis using ICA identified three distinct sources of BP_{ND}, indicating lower intensity of a striatopallidal source and greater intensity of a pallidonigral source in CUD. These source-based patterns of BP_{ND} suggest cocaine-related alterations in D_2R and D_3R may not be limited to the dorsal striatum and midbrain respectively, but may extend into the pallidum and ventral striatum. Furthermore, the alterations in striatopallidal and pallidonigral sources were associated with duration of cocaine use, and may indicate reciprocal and compensatory mechanisms of dopaminergic function in addiction. Additional investigation into concurrent alterations in D_2-like dopamine receptor systems (e.g., prior to drug exposure, during initial use and withdrawal, and following extended abstinence) should provide important insight into treatment development efforts for CUD.

Supplementary Material

Refer to Web version on PubMed Central for supplementary material.

Acknowledgments

Dr. Potenza has received financial support or compensation for the following: Dr. Potenza has consulted for and advised Boehringer Ingelheim, Ironwood, Lundbeck, INSYS, Shire, RiverMend Health and Lakelight Therapeutics/Opiant; has received research support from the NIH, Veteran's Administration, Mohegan Sun Casino, the National Center for Responsible Gaming, and Pfizer, Forest Laboratories, Ortho-McNeil, Psyadon, Oy-Control/Biotie and Glaxo-SmithKline pharmaceuticals; has participated in surveys, mailings or telephone consultations related to drug addiction, impulse control disorders or other health topics; has consulted for law offices and gambling entities on issues related to impulse control disorders; provides clinical care in the Connecticut Department of Mental Health and Addiction Services Problem Gambling Services Program; has performed grant reviews for the NIH and other agencies; has edited journals and journal sections; has given academic lectures in grand rounds, CME events and other clinical or scientific venues; and has generated books or book chapters for publishers of mental health texts. Dr. Carson has received research funding from Astellas, Astra Zeneca, BMS, Lilly, Pfizer, Taisho, and UCB.

This research was funded by the National Institute on Drug Abuse (NIDA) (P20-DA027844, R03-DA027456). Additional financial support was provided by NIDA (T32-DA022975, K12 DA00167), the National Institute of Health (NIH) (P20GM103472, R01EB005846), the State of Connecticut Department of Mental Health and Addiction Services and the National Center on Addiction and Substance Abuse. This publication was also made possible by CTSA Grant Number UL1 TR000142 from the National Center for Advancing Translational Science (NCATS), a component of NIH. Its contents are solely the responsibility of the authors and do not necessarily represent the official view of the funding agencies.

References

1. Volkow ND, Fowler JS, Wolf AP, Schlyer D, Shiue C-Y, Alpert R, et al. Effects of chronic cocaine abuse on postsynaptic dopamine receptors. Am J Psychiatry. 1990; 147:719–724. [PubMed: 2343913]
2. Volkow N, Wang G-J, Fowler J, Logan J, Gatley S, Hitzemann R, et al. Decreased striatal dopaminergic responsiveness in detoxified cocaine-dependent subjects. Nature. 1997; 386:830–833. [PubMed: 9126741]
3. Martinez D, Broft A, Foltin RW, Slifstein M, Hwang D-R, Huang Y, et al. Cocaine dependence and d2 receptor availability in the functional subdivisions of the striatum: relationship with cocaine-seeking behavior. Neuropsychopharmacology. 2004; 29:1190–1202. [PubMed: 15010698]

4. Martinez D, Narendran R, Foltin RW, Slifstein M, Hwang D-R, Broft A, et al. Amphetamine-induced dopamine release: markedly blunted in cocaine dependence and predictive of the choice to self-administer cocaine. Am J Psychiatry. 2007; 164:622–629. [PubMed: 17403976]
5. Volkow N, Tomasi D, Wang G, Logan J, Alexoff D, Jayne M, et al. Stimulant-induced dopamine increases are markedly blunted in active cocaine abusers. Mol Psychiatry. 2014; 19:1037–1043. [PubMed: 24912491]
6. Volkow N, Wang G-J, Fowler J, Logan J, Hitzemann R, Gatley S, et al. Cocaine uptake is decreased in the brain of detoxified cocaine abusers. Neuropsychopharmacology. 1996; 14:159–168. [PubMed: 8866699]
7. Narendran R, Lopresti BJ, Martinez D, Scott N, Himes M, May MA, et al. In vivo evidence for reduced striatal vesicular monoamine transporter (VMAT2) availability in cocaine abusers. Am J Psychiatry. 2012; 169:55–63. [PubMed: 22193525]
8. Matuskey D, Gallezot J-D, Pittman B, Williams W, Wanyiri J, Gaiser E, et al. Dopamine D3 receptor alterations in cocaine-dependent humans imaged with [11C](+)PHNO. Drug Alcohol Depend. 2014; 139:100–105. [PubMed: 24717909]
9. Payer DE, Behzadi A, Kish SJ, Houle S, Wilson AA, Rusjan PM, et al. Heightened D3 dopamine receptor levels in cocaine dependence and contributions to the addiction behavioral phenotype: a positron emission tomography study with [11C]-+-PHNO. Neuropsychopharmacology. 2014; 39:321–328.
10. Pérez-Mañá C, Castells X, Vidal X, Casas M, Capellà D. Efficacy of indirect dopamine agonists for psychostimulant dependence: a systematic review and meta-analysis of randomized controlled trials. J Subst Abuse Treat. 2011; 40:109–122. [PubMed: 21036508]
11. Minozzi S, Amato L, Pani P, Solimini R, Vecchi S, De Crescenzo F, et al. Dopamine agonists for the treatment of cocaine dependence. The Cochrane Database of Systematic Reviews. 2015:CD003352. [PubMed: 26014366]
12. Erritzoe D, Tziortzi A, Bargiela D, Colasanti A, Searle GE, Gunn RN, et al. In vivo imaging of cerebral dopamine D3 receptors in alcoholism. Neuropsychopharmacology. 2014; 39:1703–1712. [PubMed: 24469594]
13. Martinez D, Gil R, Slifstein M, Hwang D-R, Huang Y, Perez A, et al. Alcohol dependence is associated with blunted dopamine transmission in the ventral striatum. Biol Psychiatry. 2005; 58:779–786. [PubMed: 16018986]
14. Fehr C, Yakushev I, Hohmann N, Buchholz H-G, Landvogt C, Deckers H, et al. Association of low striatal dopamine D2 receptor availability with nicotine dependence similar to that seen with other drugs of abuse. Am J Psychiatry. 2008; 165:507–514. [PubMed: 18316420]
15. Martinez D, Saccone PA, Liu F, Slifstein M, Orlowska D, Grassetti A, et al. Deficits in dopamine D2 receptors and presynaptic dopamine in heroin dependence: commonalities and differences with other types of addiction. Biol Psychiatry. 2012; 71:192–198. [PubMed: 22015315]
16. Volkow ND, Chang L, Wang G-J, Fowler JS, Ding Y-S, Sedler M, et al. Low level of brain dopamine D2 receptors in methamphetamine abusers: association with metabolism in the orbitofrontal cortex. Am J Psychiatry. 2001; 158:2015–2021. [PubMed: 11729018]
17. Boileau I, Payer D, Rusjan PM, Houle S, Tong J, McCluskey T, et al. Heightened dopaminergic response to amphetamine at the D3 dopamine receptor in methamphetamine users. Neuropsychopharmacology. 2016; 41:2994–3002. [PubMed: 27353309]
18. Self DW. Dopamine receptor subtypes in reward and relapse. The Dopamine Receptors. 2010
19. Doherty JM, Masten VL, Powell SB, Ralph RJ, Klamer D, Low MJ, et al. Contributions of dopamine D1, D2, and D3 receptor subtypes to the disruptive effects of cocaine on prepulse inhibition in mice. Neuropsychopharmacology. 2008; 33:2648–2656. [PubMed: 18075489]
20. Banasikowski TJ, Bespalov A, Drescher K, Behl B, Unger L, Haupt A, et al. Double dissociation of the effects of haloperidol and the dopamine D3 receptor antagonist ABT-127 on acquisition vs. expression of cocaine-conditioned activity in rats. J Pharmacol Exp Ther. 2010; 335:506–515. [PubMed: 20724485]
21. Watson DJ, Loiseau F, Ingallinesi M, Millan MJ, Marsden CA, Fone KC. Selective blockade of dopamine D3 receptors enhances while D2 receptor antagonism impairs social novelty

discrimination and novel object recognition in rats: a key role for the prefrontal cortex. Neuropsychopharmacology. 2012; 37:770–786. [PubMed: 22030711]

22. Boileau I, Payer D, Houle S, Behzadi A, Rusjan PM, Tong J, et al. Higher binding of the dopamine D3 receptor-preferring ligand [11C]-(+)-propyl-hexahydro-naphtho-oxazin in methamphetamine polydrug users: a positron emission tomography study. J Neurosci. 2012; 32:1353–1359. [PubMed: 22279219]
23. Gurevich EV, Joyce JN. Distribution of dopamine D3 receptor expressing neurons in the human forebrain: comparison with D2 receptor expressing neurons. Neuropsychopharmacology. 1999; 20:60–80. [PubMed: 9885786]
24. Tziortzi AC, Searle GE, Tzimopoulou S, Salinas C, Beaver JD, Jenkinson M, et al. Imaging dopamine receptors in humans with [11C]-(+)-PHNO: dissection of D3 signal and anatomy. Neuroimage. 2011; 54:264–277. [PubMed: 20600980]
25. Searle GE, Beaver JD, Tziortzi A, Comley RA, Bani M, Ghibellini G, et al. Mathematical modelling of [11C]-(+)-PHNO human competition studies. Neuroimage. 2013; 68:119–132. [PubMed: 23207573]
26. Narendran R, Martinez D, Mason NS, Lopresti BJ, Himes ML, Chen CM, et al. Imaging of dopamine D2/3 agonist binding in cocaine dependence: a [11C] NPA positron emission tomography study. Synapse. 2011; 65:1344–1349. [PubMed: 21780185]
27. Freedman SB, Patel S, Marwood R, Emms F, Seabrook GR, Knowles MR, et al. Expression and pharmacological characterization of the human D3 dopamine receptor. J Pharmacol Exp Ther. 1994; 268:417–426. [PubMed: 8301582]
28. Gallezot JD, Beaver JD, Gunn RN, Nabulsi N, Weinzimmer D, Singhal T, et al. Affinity and selectivity of [11C]-(+)-PHNO for the D3 and D2 receptors in the rhesus monkey brain in vivo. Synapse. 2012; 66:489–500. [PubMed: 22213512]
29. Rabiner EA, Slifstein M, Nobrega J, Plisson C, Huiban M, Raymond R, et al. In vivo quantification of regional dopamine-D3 receptor binding potential of (+)-PHNO: Studies in non-human primates and transgenic mice. Synapse. 2009; 63:782–793. [PubMed: 19489048]
30. Searle G, Beaver JD, Comley RA, Bani M, Tziortzi A, Slifstein M, et al. Imaging dopamine D3 receptors in the human brain with positron emission tomography, [11C]PHNO, and a selective D3 receptor antagonist. Biol Psychiatry. 2010; 68:392–399. [PubMed: 20599188]
31. Graff-Guerrero A, Redden L, Abi-Saab W, Katz DA, Houle S, Barsoum P, et al. Blockade of [11C](+)-PHNO binding in human subjects by the dopamine D3 receptor antagonist ABT-925. International Journal of Neuropsychopharmacology. 2010; 13:273–287. [PubMed: 19751545]
32. Matuskey D, Gaiser EC, Gallezot J-D, Angarita GA, Pittman B, Nabulsi N, et al. A preliminary study of dopamine D2/3 receptor availability and social status in healthy and cocaine dependent humans imaged with [11C](+)PHNO. Drug Alcohol Depend. 2015; 154:167–173. [PubMed: 26164205]
33. First, MB., Spitzer, RL., Miriam, G., Williams, JBW. Structured Clinical Interview for DSM-IV-TR Axis I Disorders, Research Version, Patient Edition. (SCID-I/P). New York: Biometrics Research, New York State Psychiatric Institute; 2002.
34. Sheehan D, Lecrubier Y, Sheehan K, Amorim P, Janavs J, Weiller E, et al. The validity of Mini International Neuropsychiatric Interview (MINI): The development and validation of a structured diagnostic interview for DSM-IV and ICD-10. J Clin Psychiatry. 1998; 59:211–232.
35. Gallezot J-D, Zheng M-Q, Lim K, Lin S-f, Labaree D, Matuskey D, et al. Parametric imaging and test–retest variability of 11C-(+)-PHNO binding to D2/D3 dopamine receptors in humans on the high-resolution research tomograph PET Scanner. J Nucl Med. 2014; 55:960–966. [PubMed: 24732151]
36. Wilson AA, McCormick P, Kapur S, Willeit M, Garcia A, Hussey D, et al. Radiosynthesis and Evaluation of [11C]-(+)-4-Propyl-3, 4, 4a, 5, 6, 10b-hexahydro-2 H-naphtho [1, 2-b][1, 4] oxazin-9-ol as a Potential Radiotracer for in Vivo Imaging of the Dopamine D2 High-Affinity State with Positron Emission Tomography. J Med Chem. 2005; 48:4153–4160. [PubMed: 15943487]

37. Carson, RE., Barker, WC., Liow, J-S., Johnson, C. Design of a motion-compensation OSEM list-mode algorithm for resolution-recovery reconstruction for the HRRT. Nuclear Science Symposium Conference Record; IEEE; 2003. p. 3281-3285.
38. Wu Y, Carson RE. Noise reduction in the simplified reference tissue model for neuroreceptor functional imaging. J Cereb Blood Flow Metab. 2002; 22:1440–1452. [PubMed: 12468889]
39. Gallezot J-D, Matuskey D, Lim K, Zheng M, Lin S-f, Ding Y-S, et al. [11C] PHNO parametric imaging and test-retest study in humans using the HRRT scanner. J Nucl Med. 2011; 52:393–393. [PubMed: 21321269]
40. Mazziotta J, Toga A, Evans A, Fox P, Lancaster J, Zilles K, et al. A probabilistic atlas and reference system for the human brain: International Consortium for Brain Mapping (ICBM). Philos Trans R Soc Lond B Biol Sci. 2001; 356:1293–1322. [PubMed: 11545704]
41. Ashburner J, Friston KJ. Unified segmentation. Neuroimage. 2005; 26:839–851. [PubMed: 15955494]
42. Mawlawi O, Martinez D, Slifstein M, Broft A, Chatterjee R, Hwang D-R, et al. Imaging human mesolimbic dopamine transmission with positron emission tomography: I. Accuracy and precision of D2 receptor parameter measurements in ventral striatum. J Cereb Blood Flow Metab. 2001; 21:1034–1057. [PubMed: 11524609]
43. Xu L, Groth KM, Pearlson G, Schretlen DJ, Calhoun VD. Source-based morphometry: The use of independent component analysis to identify gray matter differences with application to schizophrenia. Hum Brain Mapp. 2009; 30:711–724. [PubMed: 18266214]
44. Li YO, Adali T, Calhoun VD. Estimating the number of independent components for functional magnetic resonance imaging data. Hum Brain Mapp. 2007; 28:1251–1266. [PubMed: 17274023]
45. Bell AJ, Sejnowski TJ. An information-maximization approach to blind separation and blind deconvolution. Neural Comput. 1995; 7:1129–1159. [PubMed: 7584893]
46. Caravaggio F, Raitsin S, Gerretsen P, Nakajima S, Wilson A, Graff-Guerrero A. Ventral striatum binding of a dopamine D 2/3 receptor agonist but not antagonist predicts normal body mass index. Biol Psychiatry. 2015; 77:196–202. [PubMed: 23540907]
47. Matuskey D, Worhunksy P, Correa E, Pittman B, Gallezot J-D, Nabulsi N, et al. Age-related changes in binding of the D2/3 receptor radioligand [11C](+)PHNO in healthy volunteers. NeuroImage. 2016
48. Nakajima S, Caravaggio F, Boileau I, Chung JK, Plitman E, Gerretsen P, et al. Lack of age-dependent decrease in dopamine D3 receptor availability: A [11C]-(+)-PHNO and [11C]-raclopride positron emission tomography study. J Cereb Blood Flow Metab. 2015; 35:1812–1818. [PubMed: 26058690]
49. Gaiser, EC., Jastreboff, AM., Pittman, B., Gallezot, JD., Angarita, GA., Kantrovitz, L., et al. Body mass index relationships with dopamine D3 receptor availability as measured by [11C](+)PHNO; Society for Biological Psychiatry 70th Annual Scientific Meeting; Toronto, Canada. 2015.
50. Lee B, London ED, Poldrack RA, Farahi J, Nacca A, Monterosso JR, et al. Striatal dopamine d2/d3 receptor availability is reduced in methamphetamine dependence and is linked to impulsivity. J Neurosci. 2009; 29:14734–14740. [PubMed: 19940168]
51. Martinez D, Carpenter KM, Liu F, Slifstein M, Broft A, Friedman AC, et al. Imaging dopamine transmission in cocaine dependence: link between neurochemistry and response to treatment. Am J Psychiatry. 2011; 168:634–641. [PubMed: 21406463]
52. Nader MA, Morgan D, Gage HD, Nader SH, Calhoun TL, Buchheimer N, et al. PET imaging of dopamine D2 receptors during chronic cocaine self-administration in monkeys. Nat Neurosci. 2006; 9:1050–1056. [PubMed: 16829955]
53. Conrad KL, Ford K, Marinelli M, Wolf ME. Dopamine receptor expression and distribution dynamically change in the rat nucleus accumbens after withdrawal from cocaine self-administration. Neuroscience. 2010; 169:182–194. [PubMed: 20435100]
54. Neisewander JL, Fuchs RA, Tran-Nguyen LT, Weber SM, Coffey GP, Joyce JN. Increases in dopamine D3 receptor binding in rats receiving a cocaine challenge at various time points after cocaine self-administration: implications for cocaine-seeking behavior. Neuropsychopharmacology. 2004; 29:1479–1487. [PubMed: 15100700]

55. Volkow ND, Koob G, Baler R. Biomarkers in substance use disorders. ACS Chem Neurosci. 2015; 6:522–525. [PubMed: 25734247]
56. Ferguson SM, Eskenazi D, Ishikawa M, Wanat MJ, Phillips PE, Dong Y, et al. Transient neuronal inhibition reveals opposing roles of indirect and direct pathways in sensitization. Nat Neurosci. 2011; 14:22–24. [PubMed: 21131952]
57. Hikida T, Yawata S, Yamaguchi T, Danjo T, Sasaoka T, Wang Y, et al. Pathway-specific modulation of nucleus accumbens in reward and aversive behavior via selective transmitter receptors. Proc Natl Acad Sci USA. 2013; 110:342–347. [PubMed: 23248274]
58. Kravitz AV, Tye LD, Kreitzer AC. Distinct roles for direct and indirect pathway striatal neurons in reinforcement. Nat Neurosci. 2012; 15:816–818. [PubMed: 22544310]
59. Bock R, Shin JH, Kaplan AR, Dobi A, Markey E, Kramer PF, et al. Strengthening the accumbal indirect pathway promotes resilience to compulsive cocaine use. Nat Neurosci. 2013; 16:632–638. [PubMed: 23542690]
60. Kalivas PW, Volkow ND. The neural basis of addiction: a pathology of motivation and choice. Am J Psychiatry. 2005; 162:1403–1413. [PubMed: 16055761]
61. Robinson M, Fischer A, Ahuja A, Lesser E, Maniates H. Roles of “wanting” and “liking” in motivating behavior: gambling, food, and drug addictions. Curr Top Behav Neurosci. 2015:1–32.
62. Buckholtz JW, Treadway MT, Cowan RL, Woodward ND, Li R, Ansari MS, et al. Dopaminergic network differences in human impulsivity. Science. 2010; 329:532–532. [PubMed: 20671181]
63. Staley JK, Mash DC. Adaptive increase in D3 dopamine receptors in the brain reward circuits of human cocaine fatalities. J Neurosci. 1996; 16:6100–6106. [PubMed: 8815892]
64. Negus SS, Henningfield J. Agonist medications for the treatment of cocaine use disorder. Neuropsychopharmacology. 2014; 40:1815–1825. [PubMed: 25563633]
65. Caine SB, Thomsen M, Barrett AC, Collins GT, Grundt P, Newman AH, et al. Cocaine self-administration in dopamine D3 receptor knockout mice. Exp Clin Psychopharmacol. 2012; 20:352–363. [PubMed: 22867038]
66. Cheung TH, Loriaux AL, Weber SM, Chandler KN, Lenz JD, Schaan RF, et al. Reduction of cocaine self-administration and D3 receptor-mediated behavior by two novel dopamine D3 receptor-selective partial agonists, OS-3-106 and WW-III-55. J Pharmacol Exp Ther. 2013; 347:410–423. [PubMed: 24018640]
67. Mello NK, Fivel PA, Kohut SJ, Bergman J. Effects of chronic buspirone treatment on cocaine self-administration. Neuropsychopharmacology. 2013; 38:455–467. [PubMed: 23072835]
68. Caine SB, Negus SS, Mello NK, Patel S, Bristow L, Kulagowski J, et al. Role of dopamine D2-like receptors in cocaine self-administration: studies with D2 receptor mutant mice and novel D2 receptor antagonists. J Neurosci. 2002; 22:2977–2988. [PubMed: 11923462]
69. David V, Durkin TP, Cazala P. Differential effects of the dopamine D2/D3 receptor antagonist sulpiride on self-administration of morphine into the ventral tegmental area or the nucleus accumbens. Psychopharmacology. 2002; 160:307–317. [PubMed: 11889500]
70. Abou-Elseoud A, Starck T, Remes J, Nikkinen J, Tervonen O, Kiviniemi V. The effect of model order selection in group PICA. Hum Brain Mapp. 2010; 31:1207–1216. [PubMed: 20063361]
71. Zald DH, Woodward ND, Cowan RL, Riccardi P, Ansari MS, Baldwin RM, et al. The interrelationship of dopamine D2-like receptor availability in striatal and extrastriatal brain regions in healthy humans: a principal component analysis of [18 F] fallypride binding. Neuroimage. 2010; 51:53–62. [PubMed: 20149883]
72. Zuendorf G, Kerrouche N, Herholz K, Baron JC. Efficient principal component analysis for multivariate 3D voxel-based mapping of brain functional imaging data sets as applied to FDG-PET and normal aging. Hum Brain Mapp. 2003; 18:13–21. [PubMed: 12454908]

Highlights

- [^{11}C]-(+)-PHNO binding potential reflects the relative local availability of both D_2 and D_3 receptors
- Regional analysis indicated alterations in D_2R-rich and D_3R-rich regions in cocaine-use disorder
- ICA identified source-based patterns of receptor availability consistent with DA circuitry
- Source intensities suggest CUD-related differences may also be present in D_2R/D_3R-mixed regions

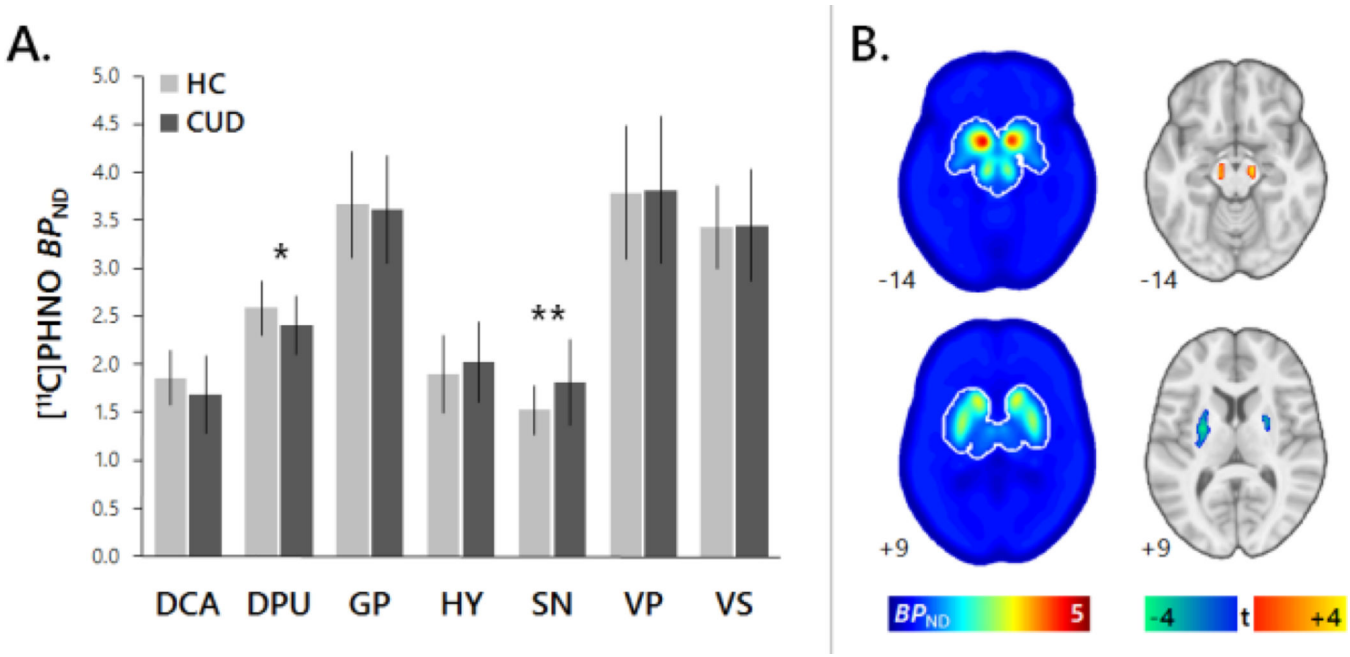

Figure 1.

Regional analyses of [^{11}C]-(+)-PHNO BP_{ND}. (**a**) Region of interest (ROI) analysis performed on smoothed parametric images. CUD relative to HC participants displayed reduced BP_{ND} in the dorsal putamen (DPU; *p<0.05) and greater BP_{ND} in the substantia nigra (SN, **p<0.01). Error bars indicate SD. (**b**) Whole-brain mean BP_{ND} across all participants with relative threshold mask borders used in GLM and ICA analyses indicated by the white outline (left) and GLM-identified regions of group differences in [^{11}C]-(+)-PHNO BP_{ND} (right). CUD relative to HC exhibited greater BP_{ND} in midbrain regions (red/yellow) and reduced BP_{ND} in the putamen (blue/green). Axial slices displayed at p<0.005, k>20 on MNI152. Abbreviations: DCA, dorsal caudate; DPU, dorsal putamen; GP, globus pallidus; HY, hypothalamus; SN, substantia nigra; VP, ventral pallidum; VS, ventral striatum.

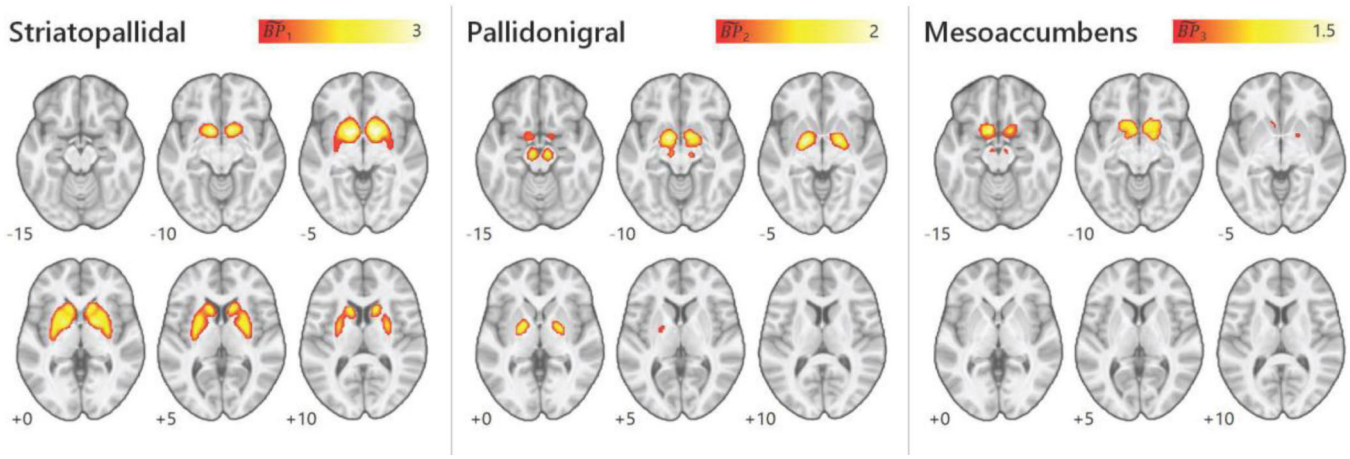

Figure 2.
ICA-identified sources of [^{11}C]-(+)-PHNO BP_{ND} displayed at $\tilde{BP}_M \geq 0.5$ on different intensity scales as denoted in the color bars.

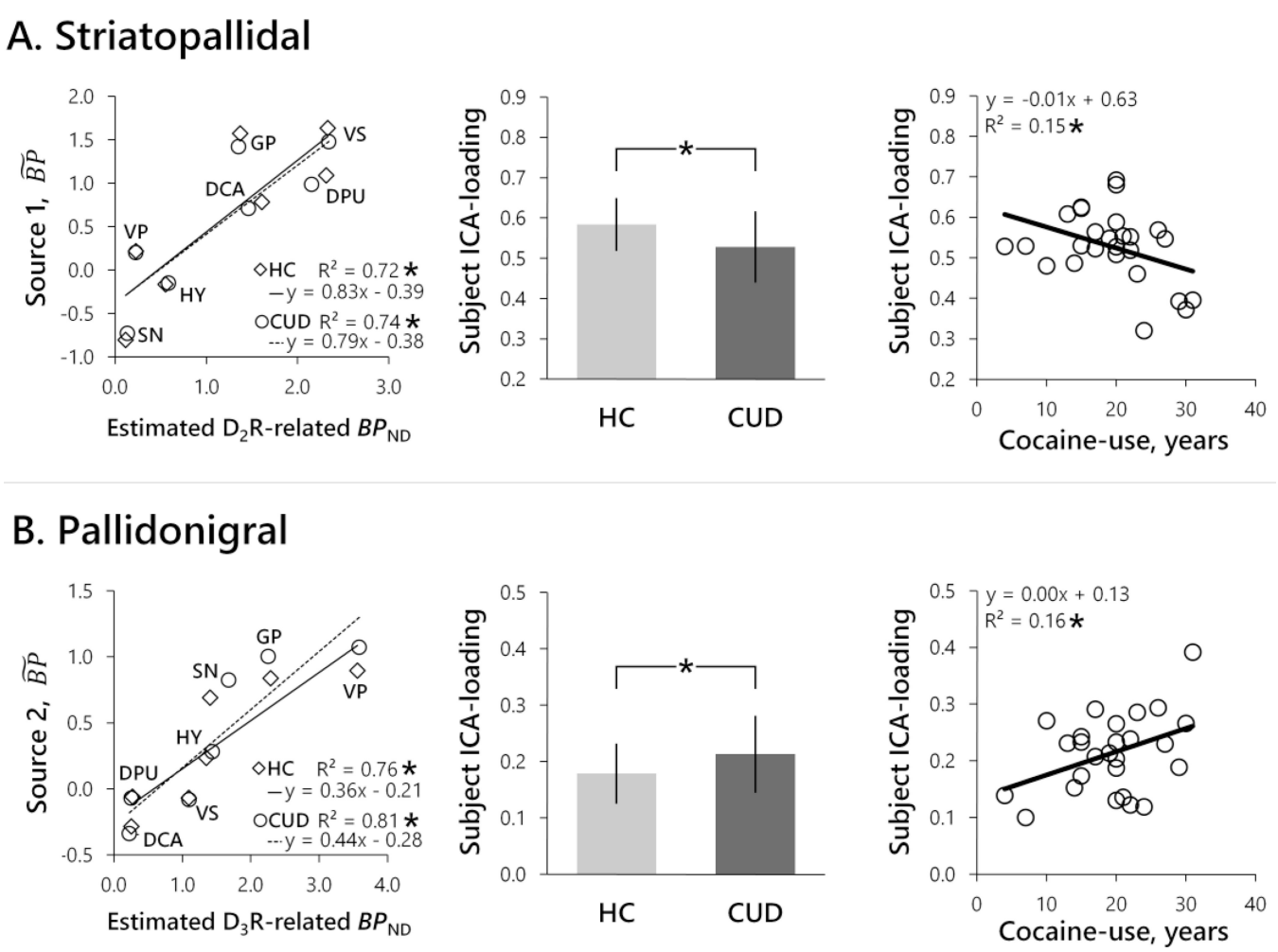

Figure 3.

Source associations with estimated regional D_2R-related and D_3R-related BP_{ND} proportions, group intensity differences and correlation with years of cocaine use for the (**a**) striatopallidal and (**b**) pallidonigral sources. Regional estimates of D_2R-related and D_3R-related BP_{ND} were calculated using reported fractions of [^{11}C]-(+)-PHNO BP_{ND} (24, 25) (see Section 2.5). Subject ICA-loadings refer to the mixing parameter representing source intensity, or how strongly each source contributed to the aggregate BP_{ND} signal. Error bars indicate SD. *p<0.05.

Table 1

Sample characteristics and injection data.

Variable	HC (N=26)	CUD (N=26)	p-value
Age, years (SD)	41.3 (6.9)	42.7 (6.4)	0.46
Gender, F (%)	5 (19.2)	5 (19.2)	1.00
Body-mass, BMI (SD)	28.7 (6.0)	29.9 (6.5)	0.47
Daily tobacco user, N (%)	1 (3.8)	22 (84.6)	<0.001
Daily tobacco use, cigarettes (SD)	0.4 (2.0)	9.2 (6.4)	<0.001
Weekly alcohol use, drinks (SD)	1.4 (2.2)	6.8 (14.6)	0.75
Amount of cocaine per use, $ (SD)	-	112.7 (148.5)	-
Frequency of use, days/month (SD)	-	19.0 (7.7)	-
Last cocaine use before PET, days (SD)	-	7.8 (4.9)	-
CUD chronicity, years (SD)	-	19.3 (6.3)	-
Radioactive dose, MBq (SD)	398 (155)	370 (146)	0.51
Injected mass, μg/kg (SD)	0.024 (0.007)	0.025 (0.006)	0.63
Specific activity, MBq/nmol (SD)	56.7 (30.3)	46.9 (19.5)	0.17

Table 2

Regional composition of sources of [^{11}C]-(+)-PHNO BP_{ND}.

Component/region	k	x	y	z	peak $\tilde{B}PM_M$
a. Striatopallidal					
L DPU, DCA, GP, VP, VS	1467	−10	8	−8	3.20
R DPU, DCA, GP, VP, VS	1416	14	6	−4	3.06
b. Pallidonigral					
R GP, HY, SN, VP	457	12	2	−10	1.60
L GP, HY, SN, VP	579	−14	−2	−8	1.97
c. Mesoaccumbens					
R SN	5	10	−14	−16	0.59
L SN	6	−6	−12	−16	0.62
R HY, VP, VS	243	10	10	−12	1.23
L HY, VP, VS	259	−8	8	−14	1.39

Regional composition of ICA-identified sources at the threshold of ICA-estimated BP_{ND} contribution ($\tilde{B}P_M$) ≥0.5. Cluster information includes spatial extent (k, in voxels), peak location (x, y, z) in MNI152 space and peak $\tilde{B}P_M$.

Abbreviations: DCA, dorsal caudate; DPU, dorsal putamen; GP, globus pallidus; HY, hypothalamus; SN, substantia nigra; VP, ventral pallidum; VS, ventral striatum; R/L, right/left hemisphere.